Arch Toxicol
DOI 10.1007/s00204-015-1486-9

ORGAN TOXICITY AND MECHANISMS

# Polyhexamethylene guanidine phosphate aerosol particles induce pulmonary inflammatory and fibrotic responses

**Ha Ryong Kim · Kyuhong Lee · Chang We Park · Jeong Ah Song · Da Young Shin · Yong Joo Park · Kyu Hyuck Chung**

Received: 1 August 2014 / Accepted: 12 February 2015


**Abstract** Polyhexamethylene guanidine (PHMG) phosphate was used as a disinfectant for the prevention of microorganism growth in humidifiers, without recognizing that a change of exposure route might cause significant health effects. Epidemiological studies reported that the use of humidifier disinfectant containing PHMG-phosphate can provoke pulmonary fibrosis. However, the pulmonary toxicity of PHMG-phosphate aerosol particles is unknown yet. This study aimed to elucidate the toxicological relationship between PHMG-phosphate aerosol particles and pulmonary fibrosis. An in vivo nose-only exposure system and an in vitro air–liquid interface (ALI) co-culture model were applied to confirm whether PHMG-phosphate induces inflammatory and fibrotic responses in the respiratory tract. Seven-week-old male Sprague–Dawley rats were exposed to PHMG-phosphate aerosol particles for 3 weeks and recovered for 3 weeks in a nose-only exposure chamber. In addition, three human lung cells (Calu-3, differentiated THP-1 and HMC-1 cells) were cultured at ALI condition for 12 days and were treated with PHMG-phosphate at set concentrations and times. The reactive oxygen species (ROS) generation, airway barrier injuries and inflammatory and fibrotic responses were evaluated in vivo and in vitro. The rats exposed to PHMG-phosphate aerosol particles in nanometer size showed pulmonary inflammation and fibrosis including inflammatory cytokines and fibronectin mRNA increase, as well as histopathological changes. In addition, PHMG-phosphate triggered the ROS generation, airway barrier injuries and inflammatory responses in a bronchial ALI co-culture model. Those results demonstrated that PHMG-phosphate aerosol particles cause pulmonary inflammatory and fibrotic responses. All features of fibrogenesis by PHMG-phosphate aerosol particles closely resembled the pathology of fibrosis that was reported in epidemiological studies. Finally, we expected that PHMG-phosphate infiltrated into the lungs in the form of aerosol particles would induce an airway barrier injury via ROS, release fibrotic inflammatory cytokines, and trigger a wound-healing response, leading to pulmonary fibrosis. A simultaneous state of tissue destruction and inflammation caused by PHMG-phosphate had whipped up a "perfect storm" in the respiratory tract.

**Keywords** Polyhexamethylene guanidine phosphate · Aerosol particles · Humidifier disinfectant · Pulmonary fibrosis

## Introduction

Many people use various chemicals in their houses to improve hygiene and esthetics, and it is highly likely that the indoor air is contaminated with those chemicals. Although the safety of these chemicals has been proven by registering them with regulatory to support the public health protection, there is still a risk of inhaled exposure

Ha Ryong Kim and Kyuhong Lee have contributed equally to this work.

H. R. Kim · C. W. Park · D. Y. Shin · Y. J. Park · K. H. Chung (✉)
School of Pharmacy, Sungkyunkwan University, Suwon 440-746, Korea
e-mail: khchung@skku.edu

K. Lee · J. A. Song
Inhalation Toxicology Research Center, Korea Institute of Toxicology, Jeongeup 580-185, Korea

K. Lee
Human and Environment Toxicology, University of Science and Technology, Daejeon 305-350, Korea

Published online: 26 February 2015

to household chemicals. Several clinical studies have reported respiratory disorders after the accidental inhalation of household sprays used for cleaning or waterproofing (Gorguner et al. 2004; Heinzer et al. 2004). In addition, epidemiological studies have suggested that frequent use of household cleaning sprays may be an important risk factor for asthma (Zock et al. 2007).

In Korea, manufacturers have extended the use of disinfectants to humidifier water to prevent the growth of harmful bacteria, mold and algae. They are called "humidifier disinfectant" products. However, epidemiological studies reported that the use of humidifier disinfectants can provoke a fatal lung disease, which is pathologically characterized by a sub-acute destructive and obliterative bronchiolitis and subsequent massive fibrosis (Kim et al. 2014a, b; Hong et al. 2014). In general, the humidifier generates a visible fog with micrometers in size; however, previous studies showed that humidifiers may release dissolved particles that are nanometers in size (Rodes et al. 1990; Umezawa et al. 2013). Such particles could easily penetrate into the deep air spaces of the respiratory tract. Therefore, adding the disinfectants to humidifier water may allow a lot of aerosolized of disinfectant particles to penetrate deep into the lungs. Polyhexamethylene guanidine (PHMG) phosphate, one of the humidifier disinfectants, has been suggested as a causative chemical of fatal lung disease (KCDC 2011).

PHMG-phosphate comprises the polymeric guanidine family, which are cationic antimicrobial agents with a broad spectrum of activity against gram-positive and gram-negative bacteria (Gilbert and Moore 2005; Oulé et al. 2012). This agent has been registered as disinfectant of medical devices by the United States Food and Drug Administration. PHMG-phosphate has a competitive advantage among the polymeric guanidine family because of its stronger bacteriostatic activity against some strains and a high threshold of skin-irritating, neurotoxic and chronic effects (Aleshina et al. 2001). However, the toxicity of PHMG-phosphate has been reported recently. The treatment of zebrafish with PHMG-phosphate resulted in acute cardiovascular toxicity that was associated with severe inflammation and atherogenesis (Kim et al. 2013). In particular, inhalation exposure of PHMG-phosphate induced histopathological fibrotic changes in the lung tissues of mice (Song et al. 2014). However, the fibrogenesis mechanism induced by PHMG-phosphate is currently unclear.

Pulmonary fibrosis is a disease characterized by accumulation of extracellular matrix proteins, excessive collagen deposition and matrix remodeling, which leads to an irreversible destruction of the lung architecture, lung malfunction, disruption of gas exchange and ultimately death (Wynn 2011). In general, widely different types of fibrogenic agents such as bleomycin, paraquat, radiation and asbestos fibers generate reactive oxygen species (ROS), which causes lung injuries (Bonner 2008). The ROS can provoke a disruption of the airway barrier, an important step in pulmonary fibrosis. Then, the basement membrane injury caused by a disruption of the airway barrier stimulates the over-expression of matrix metalloproteinases (MMPs) or tissue inhibitors of metalloproteinases (TIMPs). The balance of MMPs and TIMPs in the lung regulates inflammation and determines the net amount of collagen deposited during the healing response (Pardo and Selman 2006). In addition, ROS can activate macrophages and lymphocytes to produce a variety of cytokines, including pro-inflammatory cytokines, which are multifunctional and contribute to inflammatory cell recruitment and activation. A tissue injury via ROS is followed by a fibrotic repair process involving increases in transforming growth factor-beta (TGF-β) expression, increased fibronectin, collagen synthesis and a marked increase deposition of the extracellular matrix (ECM). The expression of collagens and fibronectin is up-regulated in lungs with disrupted basement membranes (Limper et al. 1991). Pulmonary fibrosis results from a dysregulation that leads to repetitive injury inflammation and collagen deposition.

There are a number of different in vivo and in vitro experimental approaches described in order to investigate the toxic effects of inhaled chemicals. Various in vivo systems have been developed to house or restrain experimental subjects. In particular, nose-only exposure systems can directly provide toxicity information of test subjects while minimizing skin or fur contamination with a highly accurate amount of the applied dose. Even though nose-only systems can create 'holding stress' due to the constraint compared with whole-body exposure systems, they are still valid ways of determining the toxicity of test article in exposed animals when compared to control animals that are exposed to filtered air without the test article. In addition, constraint training before exposure to the test article can help acclimation of animals and reduce holding stress. The use of an air–liquid interface (ALI) co-culture model of the human epithelial airway barrier composed of epithelial cells and the two most important immune cells of the lung has been established as a valid in vitro system, since in vitro studies using cultured lung cells under submerged conditions do not represent the conditions that would be expected in a human lung (Herzog et al. 2013). The heterogeneous ALI cultures of airway epithelial cells have provided a robust model system to study many aspects of the epithelial biology of airways and the pathogenesis of fibrosis (Matsui et al. 2005). The aim of the present study is to elucidate the toxicological relationship between PHMG-phosphate aerosol particles and pulmonary fibrosis. The rats were exposed to 1.51 mg/m$^3$ PHMG-phosphate aerosol particles for 3 weeks and recovered for 3 weeks in the nose-only exposure chamber. The experimental dose was

determined based on the total uptake of human exposure from an epidemiological survey (Kim et al. 2014a, b; Hong et al. 2014). The fibrotic inflammatory changes in lung tissue were analyzed. In addition, an ALI co-culture model using three human lung cell lines (Calu-3, THP-1 and HMC-1 cells) was applied to elucidate the mechanism of fibrogenesis by PHMG-phosphate. ROS generation, airway barrier injuries and profibrotic inflammatory responses were also evaluated in the ALI co-culture model.

## Materials and methods

### Nose-only exposure to PHMG-phosphate aerosol particles

The animal study protocol was approved by the Institutional Animal Care and Use Committee of the Korea Institute of Toxicology. Seven-week-old male Sprague–Dawley rats were purchased from Orient Bio (Seongnam, Korea) for the in vivo inhalation study and were acclimated for 11 days before starting the experiments. Male rats were selected to avoid the effects of the estrous cycle on toxicological responses, and because no significant differences between the genders were observed in the previous study (Song et al. 2014). Holder adaptation training was done 3 times before exposure to reduce the restraint stress. An animal room was maintained at 22 ± 3 °C with relative humidity of 50 ± 10 %, with air ventilation refreshed 10–20 times/h, and a light intensity of 150–300 Lux with a 12 h light/dark cycle. HEPA-filtered clean air was supplied to the animal room. Rats had ad libitum access to pelleted food for experimental animals (PMI Nutrition International, Richmond, IN, USA) and UV-irradiated (Steritron SX-1; Daeyoung, Seoul, Korea) and filtered (1 μm) tap water.

The PHMG-phosphate aerosol particles were generated using a nanoparticle generator (Sibata, Tokyo, Japan) in nose-only exposure chambers. The mass concentration of PHMG-phosphate aerosol particles was measured by gravimetric analysis of 25-mm glass fiber filters coated with fluorocarbon (Pallflex products, Putnam, CT, USA). The size distribution of PHMG-phosphate aerosol particles was measured using a scanning nanoparticle spectrometer (SNPS; HCT, Icheon, Korea).

Animals were randomly assigned to 2 weight-matched experimental groups by using the Path/Tox System (Version 4.2.2; Xybion Medical Systems, Cedar Knolls, NJ, USA). A nose-only exposure system was used to expose the rats to PHMG-phosphate aerosol particles. The exposure concentration (1.5 mg/m$^3$) in this study was determined based on the total uptake of human exposure from an epidemiological survey (Kim et al. 2014a, b; Hong et al. 2014). The patients used a humidifier for over 8 h a day over a 4-month period and showed the symptoms of pulmonary disease in March almost at the end of winter. The atmosphere concentration of PHMG-phosphate aerosol particles was approximately 0.1 mg/m$^3$ according to our preliminary study when the product was used as recommended (KCDC 2011). Considering the specific differences (Reagan-Shaw et al. 2008) and the respiratory physiology (Kacmarek et al. 2013) of humans and rats, the exposure concentration for rats can be calculated using the following formula (Alexander et al. 2008) with the exposure design in this study.

$$\text{Exposure concentration}\left(\frac{\text{mg}}{\text{L}}\right) = \frac{\text{Total uptake}\left(\frac{\text{mg}}{\text{kg}}\right) \times \text{Body weight (kg)}}{\text{Respiratory Minute Volume (L/min)} \times \text{duration (min)}}$$

The rats were exposed to PHMG-phosphate aerosol particles or clean air for 4 h/day for 5 days/week over a 3-week period. The rats that underwent a 3-week period of nose-only exposure were allowed to recover for 3 weeks before necropsy. Body weight was measured prior to the first exposure and two times a week thereafter, and clinical signs were observed every day. Respiration rates were measured for 10 s on days 20, 27, 35 and 42 while the animals were dormant and immobile. On day 44, the rats were euthanized by an overdose of isoflurane and necropsied. The lungs were removed and weighed. The left lungs were fixed in 10 % neutral buffered formalin (BBC biochemical, Mt Vernon, WA, USA) for histological examination. The right lungs were snap-frozen in liquid nitrogen and kept in a deep freezer until analysis for evaluation of gene expression and cytokine levels.

Total RNAs were isolated from frozen rat lungs using RNeasy Mini kit (Qiagen, Valencia, CA, USA). One μg of total RNA was reverse transcribed to cDNA with Improm-II TM Reverse Transcription System (Promega, Madison, WI, USA). The expression of fibronectin was determined using SYBR Green master mix (Applied Biosystems, Foster City, CA, USA). β-Actin was used as an internal control. The sequences of the primers: fibronectin: sense, 5′-CCCGGAACAGATGCAATGATC-3′; antisense, 5′-TGCTCCATGTGTCTCCAATTCT-3′; β-actin: sense, 5′-GCCTCACTGTCCACCTTCCA-3′; antisense, 5′-GGGCCGGACTCACG TACT-3′.

### Histopathological examination of lung tissue

The fixed lungs of the rats were embedded in paraffin blocks, prepared as microtome slices, and placed onto glass slides. All the samples were stained with hematoxylin and eosin (H&E; Sigma-Aldrich, St. Louis, MO, USA). Lungs slides were stained with Masson's trichrome staining (Sigma-Aldrich) to evaluate collagen deposition. All animal lungs were examined under light microscopy. Inflammation and fibrosis scores were evaluated on a subjective

**Table 1** Media for cell cultures

| Cell culture | Medium | Supplements |
|---|---|---|
| *Mono-culture* | | |
| Calu-3 | Dulbecco's Modified Eagle's Medium (DMEM) | L-Glutamine pyridoxine hydrochloride sodium pyruvate (110 mg/l) |
| THP-1 | Roswell Park Memorial Institute (RPMI) 1640 | L-Glutamine 25 mM HEPES buffer sodium pyruvate (110 mg/l) |
| HMC-1 | Iscove's Modified Dulbecco's Medium (IMDM) | GlutaMAX™-1 (Invitrogen, Carlsbad, CA, USA) |
| Triculture | DMEM + RPMI 1640 + IMDM 10:2:1 | |

All media were supplemented with 5 % fetal bovine serum, penicillin (100 units/ml) and streptomycin (100 μg/ml). HEPES: hydroxyethyl piperazine ethane sulfonic acid

scale of 0–5: 0 = no presence of inflammation and fibrosis, 1 = presence of inflammation and fibrosis involving <20 % of the lung parenchyma, 2 = lesions involving 20–40 % of the lung, 3 = lesions involving 40–60 % of the lung, 4 = lesions involving 60–80 % of the lung, and 5 = lesions involving >80 % of the lung.

## Preparation of bronchial ALI co-culture model

Human cell lines included Calu-3, a bronchial epithelial cell; THP-1, a monocyte cell (American Type Culture Collection, Rockville, MD, USA), which differentiated into macrophage-like cells by overnight incubation with 100 nM phorbol myristate acetate (Sigma-Aldrich), and HMC-1, a mast cell. The media for each cell culture are indicated in Table 1. Human cell lines were cultured at 37 °C in an atmosphere of 5 % $CO_2$/95 % air under saturating humidity.

Calu-3, THP-1 and HMC-1 cells were used in the bronchial ALI co-culture model, which mimics the human lung microenvironment. The epithelial cells are critical in functioning as a physical barrier. The macrophages and mast cells play the two most important roles in immune system through phagocytosis and histamine secretion, respectively. The bronchial ALI co-culture model was designed by using cell culture inserts (0.4 μm pore size, transparent polyethylene terephthalate membrane, 10.3 mm diameter, 0.9 $cm^2$ effective growth area; BD Biosciences, Erembodegem, Belgium) and its companion plates (BD Biosciences). The epithelial, macrophages and mast cells were seeded at the same time on the apical surface at a 10:2:1 ratio [epithelial cells ($1 \times 10^5$/apical); macrophages ($2 \times 10^4$/apical) and mast cells ($1 \times 10^4$/apical)] in 500 μl media according to the Alfaro-Moreno's method (2008). Two milliliters of media were added to the basolateral compartment. After 24 h, the medium in the apical chamber was removed to let cells grow in the condition of ALI and the basolateral media was changed. The medium in the basolateral chamber was changed every other day until day 12 at 37 °C in a humidified atmosphere of 5 % $CO_2$. On day 12, the airway barrier was identified by staining of mucus and was used in the following experiments. In in vitro studies, co-cultured cells at ALI were submerged with PHMG-phosphate with a concentration representing the maximum cellular response.

## Cell viability

The viability of the co-culture cells was assessed using the WST-1 method. The prepared bronchial ALI co-culture model was treated with PHMG-phosphate (SK chemicals, Suwon, Korea) at concentrations ranging from 0.3 to 70.2 mg/ml for 1, 6 and 24 h. 10 μl of Cell Proliferation Reagent WST-1 (Roche Diagnostics, Mannheim, Germany) was added to each well according to the manufacturer's instructions, and the plates were incubated in 5 % $CO_2$ at 37 °C for 4 h. Cell viability was quantified by measuring the absorbance at 440 nm using a VERSAmax microplate reader (Molecular Devices, Sunnyvale, CA, USA).

## Determination of ROS generation

The dichlorodihydrofluorescein diacetate (DCFH-DA) method was performed to determine the increase of intracellular ROS in co-culture cells treated with PHMG-phosphate. The prepared bronchial ALI co-culture model was treated with PHMG-phosphate (4.4–35.1 mg/ml) for 3 h and then loaded with DCFH-DA (Invitrogen, Carlsbad, CA, USA) for 1 h as an intracellular ROS indicator. Each well was washed twice with phosphate-buffered saline (PBS), and the cells were lysed by adding 300 μl 0.1 N NaOH for 2 min. The DCF (green fluorescence) production was measured in a model LS50B fluorometer (Perkin-Elmer, Shelton, CT, USA) with an excitation wavelength of 485 nm and an emission wavelength of 535 nm. The transwell membrane was cut out and mounted by Prolong® Gold antifade reagent (Invitrogen) to visualize the fluorescence. A Zeiss LSM 700 Laser Confocal Microscope (Thornwood, NY, USA) was used for the fluorescence observation.

### Transepithelial electrical resistance (TEER) measurement

TEER was measured with EVOM 2 Epithelial Voltohmmeter (World Precision Instruments, Sarasota, FL, USA) in order to monitor the decrease in barrier integrity caused by PHMG-phosphate in the bronchial ALI co-culture model. The cells on the apical surface were exposed for 24 h with concentrations of 0.3 to 17.6 mg/ml of PHMG-phosphate. The PHMG-phosphate was removed and once washed with PBS and then only media (500 μl) was filled in the apical chamber. The cell-free blank value was measured and subtracted for each raw value of the sample measurement. The surface area of transwell membrane (0.9 $cm^2$) was multiplied to obtain TEER (Ohm × $cm^2$).

### Immunofluorescence

In order to identify whether PHMG-phosphate affects the junctional complexes, which maintain the integrity of the airway barrier, the immunofluorescence method was performed to visualize E-cadherin in the bronchial ALI co-culture model. The apical surface was exposed to PHMG-phosphate for 24 h to analyze the destruction of E-cadherin by PHMG-phosphate. Cells were fixed with 4 % paraformaldehyde for 30 min at 37 °C. Then, cells were permeabilized with 0.1 % Triton X-100 in PBS for 10 min at 37 °C. Bovine serum albumin (BSA, 1 % w/v) in PBS (0.2 μm filtered) was used to block the cells for 1 h at 37 °C. For the primary antibody, anti-E-cadherin antibody (Abcam, Cambridge, MA, USA) diluted in 1 % w/v BSA in PBS was used and incubated with the cells for 1 h at 37 °C. For the second antibody, anti-mouse IgG FITC (Sigma-Aldrich) was diluted in BSA (1 % w/v) in PBS and incubated for 1 h at 37 °C. The transwell membrane was cut out and mounted by Prolong® Gold antifade reagent (Invitrogen, Carlsbad, CA, USA). Finally, the Zeiss LSM 700 Laser Confocal Microscope was used to observe E-cadherin fluorescence.

### Paracellular permeability test

The FITC-dextran fluxes were assessed to determine the permeability from the apical side to the basolateral side, which is caused by PHMG-phosphate in the bronchial ALI co-culture model. 40 kDa of FITC-dextran (Sigma-Aldrich) was dissolved in 1 mg/ml of *P* buffer (10 mM HEPES (pH 7.4), 1 mM sodium pyruvate, 10 mM glucose, 3 mM $CaCl_2$ and 145 mM NaCl) and added to the apical surface. After the apical surface was exposed to PHMG-phosphate (0.3 to 17.6 mg/ml) for 24 h, supernatant from the apical and the basolateral compartments were removed. 500 μl of FITC-dextran was added to the apical surface, and 2 ml of *P* buffer was added to the basolateral surface and incubated for 6 h. *P* buffer (200 μl) in basolateral chamber was collected, and the amounts of FITC-dextran were measured by LS50B fluorometer (Perkin-Elmer) with an excitation wavelength of 485 nm and an emission wavelength of 535 nm.

### Gene expression analysis

The MMPs and TIMPs are critical factors in inflammation and collagen deposition. In order to identify the changes in expression of MMPs and TIMPs mRNA by PHMG-phosphate, total RNA was isolated from co-culture cells using a Trizol reagent (Life technologies, Carlsbad, CA, USA). Total RNA (1 μg) was reverse transcribed to cDNA with AccuPower® RocketScript RT-PCR premix (Bioneer, Daejeon, Korea). The expression of genes was determined using SYBR premix Ex-Taq™ II (Takara Bio, Shiga, Japan). 18 s rRNA was used as an internal control. The sequences of the primers were as follows: MMP-2, sense, 5′-GAGAACCAAAGTCTGAAGAG-3′; antisense, 5′-GGAGTGAGAATGCTGATTAG-3′; MMP-9, sense, 5′-TTTGACAGCGACAAGAAGTGG-3′; antisense, 5′-AGGGCGAGGACCATAGAGG-3′; TIMP-1, sense, 5′-TTC CACAGGTCCCACAAC-3′; antisense, 5′-GCATTCCTCACAGCCAAC-3′; TIMP-2, sense, 5′-CCGCTCAAATACCTTCACAAT-3′; antisense, 5′-TTACGGCAGCAAGTCCAATA-3′; and 18 s rRNA, sense, 5′-TAGAGTGTTCAAAGCAGGCCC-3′; antisense, 5′-CCAACAAAATAGAACCGCGGT-3′.

### Cytokine measurement by ELISA

The tumor necrosis factor-alpha (TNF-α), interleukin (IL)-1β, IL-6, IL-8, and TGF-β play important roles in fibrotic inflammatory responses. Therefore, the levels of cytokines regulated by PHMG-phosphate were measured. Frozen lungs were weighed and placed in PBS containing 1 % Triton X-100 (100 mg tissue per milliliter), homogenized using a homogenizer (IKA, Staufen, Germany), and incubated at 4 °C for 30 min. The homogenates were centrifuged at 13,000 rpm, and supernatants were collected. Co-culture cells were exposed to PHMG-phosphate for 1, 6 and 24 h, and the medium on the apical side was collected in 1.5-ml tubes at each time point and centrifuged at 12,000×*g* for 1 min. The supernatant was collected and stored at −80 °C until use. The total protein in the homogenates was determined by the BCA protein assay (Sigma-Aldrich). The quantification of levels of TNF-α (DY210; R&D systems, Minneapolis, MN, USA), IL-1β (MLB00C; R&D systems), IL-6 (M6000B; R&D systems), IL-8 (CSB-E07274 m; Cusabio Biotech, Wuhan, China) and TGF-β (mTGF-β1; R&D systems) was conducted according to the manufacturer's protocols.

### Data analysis

The data were analyzed using Sigma Plot software (Jandel Science Software, San Rafael, CA, USA) and Excel (Microsoft, Redmond, WA, USA). Statistical analysis was performed using SPSS version 18.0 (SPSS, Chicago, IL, USA). Data from rats exposed to PHMG-phosphate aerosols were compared with sham-exposed rats using independent t test for equal and unequal variances. All in vivo data were expressed as mean ± standard error (SE). Each in vitro assay was performed at least in triplicate. The in vitro data of each assay were expressed as the mean ± standard deviation (SD). Differences between groups were assessed by Duncan's post hoc test following one-way analysis of variance. Statistical significance was accepted at $p < 0.01$ or <0.05.

## Results

### Effect of PHMG-phosphate aerosol particles on inflammation and fibrosis in rats

First, we generated PHMG-phosphate aerosol particles with nanometers in size using a nanoparticle generator.

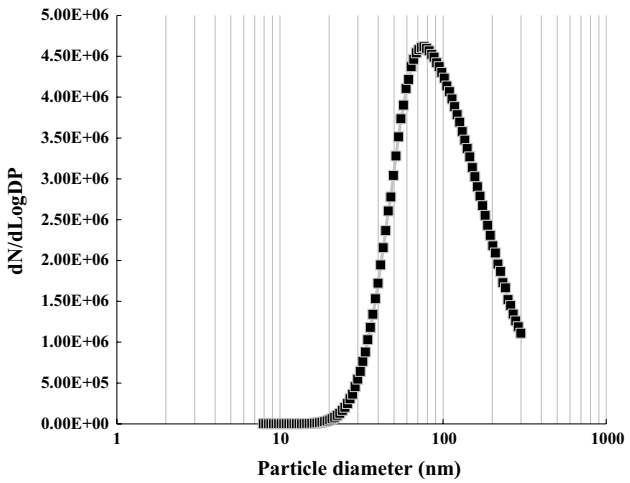


**Fig. 1** Size distributions of PHMG-phosphate aerosol particles. The PHMG-phosphate aerosol particles were analyzed by using scanning nanoparticle spectrometry

**Table 2** Physicochemical properties of PHMG-phosphate aerosol particles

| Physicochemical properties | Values[a] |
|---|---|
| Mass concentration | 1.51 ± 0.05 mg/m$^3$ |
| Size distribution | 93.35 ± 1.73 nm |

[a] Mass concentration and size distribution values are expressed as arithmetic and geometric index, respectively

**Table 3** Effect of PHMG-phosphate aerosol particles on the respiration rate in rats

| Groups | Respiration rate (frequency/minute) | | | |
|---|---|---|---|---|
| | Day 20 | Day 27 | Day 35 | Day 42 |
| Control | 80.7 ± 6.6 | 80.3 ± 3.1 | 80.0 ± 3.4 | 79.3 ± 2.2 |
| PHMG-phosphate | 208.0 ± 2.0[a] | 238.0 ± 3.4[a] | 234.0 ± 8.7[a] | 242.3 ± 7.4[a] |

[a] Mean value of the treated group was significantly different from the control group ($p < 0.05$)

The PHMG-phosphate aerosol particles had a mean diameter of 93.35 ± 1.73 nm; 56.1 % of particles were ≤100 nm in size (Fig. 1). The mass concentration of PHMG-phosphate aerosol particles was 1.51 ± 0.05 mg/m$^3$ during the exposure period in the nose-only exposure chamber (Table 2). The rats were exposed to these particles for 3 weeks and recovered for 3 weeks, considering the case of a hospitalized patient which may be injured by a humidifier disinfectant.

Piloerection, reduced movement and hunching posture were observed in the exposure group of PHMG-phosphate aerosol particles. Also, irregular respiration was observed on day 17 after exposure. As a result of measuring the respiration rate at days 20, 27, 35 and 42, rats treated with PHMG-phosphate aerosol particles showed a 2.6 times higher respiration rate than the control animals (Table 3). The rats in the exposure group gained significantly lesser body weight from day 22 (8 % loss compared with the control group), the first day after last exposure and did not recover until the end of the experiment (25 % loss compared with the control group) (Fig. 2a). In addition, the absolute and relative (lung weight/body weight) lung weights of rats treated with PHMG-phosphate aerosol particles were significantly increased to approximately 163 and 224 % compared with the control group, respectively (Fig. 2b).

The cytokines and fibronectin mRNA regulation were assessed in the lung tissues of rats exposed to PHMG-phosphate aerosol particles. The IL-1β and IL-6 were significantly up-regulated in the lung tissues of rats (Fig. 3a). The mRNA expression of fibronectin was significantly enhanced to 1.94-fold induction compared with control group (Fig. 3b).

Representative micrographs and quantitative histopathologic evaluation of lung tissues are shown in Fig. 4 and Table 4. Infiltration of inflammatory cells, such as lymphocytes and mononuclear cells, were observed in the peribronchiolar and perivascular areas of the lungs in the exposure group (Fig. 4b). Foamy histiocytes and increased alveolar macrophages were seen in the alveoli and alveolar sac (Fig. 4b, c). Bronchiolization and squamous metaplasia

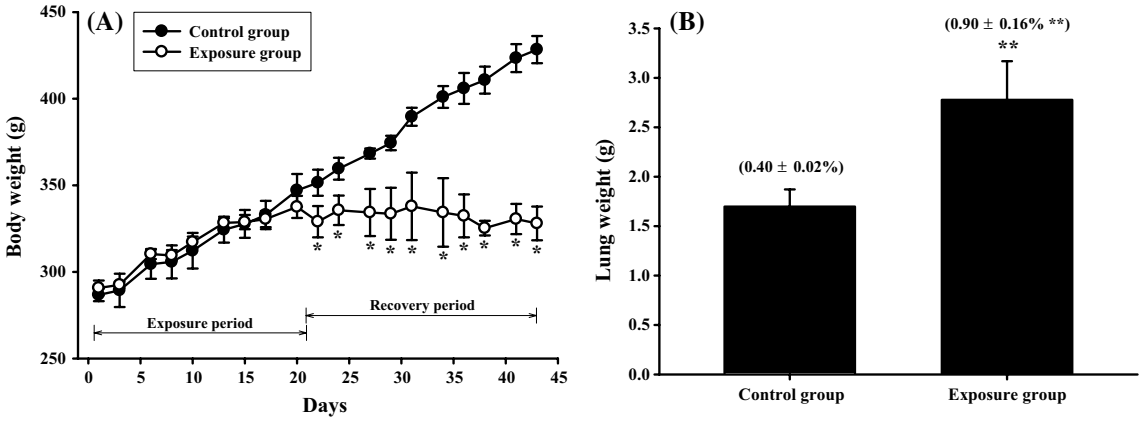


**Fig. 2** Effect of PHMG-phosphate aerosol particles on body and lung weight in rats. The body (**a**) and lung weight (**b**) of rats were expressed as mean ± SE in grams. Absolute weight of lungs is presented as black bar, and lung weight/body weight is presented in parentheses as percentage (**b**). Values are significantly different from control group: $*p < 0.05$; $**p < 0.01$

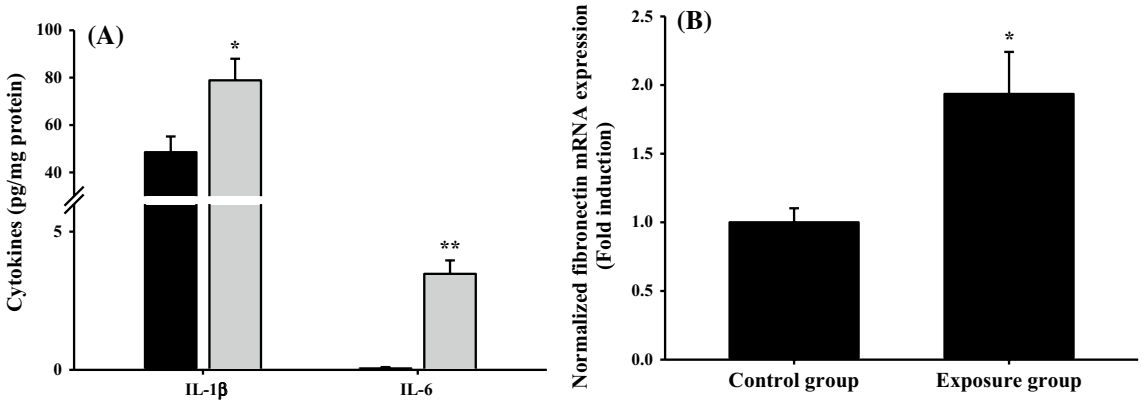


**Fig. 3** Effect of PHMG-phosphate aerosol particles on expression of the cytokines IL-1β and IL-6, and fibronectin mRNA in rats. The IL-1β and IL-6 (**a**) were measured by using cytokine ELISA kits. The IL-1β and IL-6 levels were significantly increased in rats exposed to 1.51 mg/m$^3$ PHMG-phosphate aerosol particles (*gray bar*) compared with control group (*black bar*). The fibronectin mRNA (**b**) was normalized to β-actin and calculated as fold induction. The results are expressed as mean ± SE ($n = 6$ rats/group). Values are significantly different from control group: $*p < 0.05$; $**p < 0.01$

**Table 4** Quantitative histopathologic evaluation of lung tissues of rats exposed to PHMG-phosphate aerosol particles

| Findings | Animal ID | | | | | | | | | | | |
|---|---|---|---|---|---|---|---|---|---|---|---|---|
| | 1 | 2 | 3 | 4 | 5 | 6 | 7 | 8 | 9 | 10 | 11 | 12 |
| Groups | Control | | | | | | PHMG-phosphate aerosol particles | | | | | |
| Inflammation | 0 | 0 | 0 | 0 | 0 | 0 | 2 | 2 | 2 | 2 | 2 | 2 |
| Fibrosis | 0 | 0 | 0 | 0 | 0 | 0 | 2 | 2 | 2 | 2 | 2 | 2 |

0: no symptoms; 1: minimal (<20 %); 2: slight (20–40 %); 3: moderate (40–60 %); 4: marked (60–80 %); 5: severe (>80 %)

of alveolar epithelial cells, atrophy/necrosis of bronchiolar epithelium, mucus plug in the bronchiole and congestion/hemorrhage were also identified in the lungs of rats treated with PHMG-phosphate aerosol particles (Fig. 4d). With Masson's trichrome stain, lung sections showed increased collagen accumulation, namely fibrotic change, especially in the thickened alveolar regions (Fig. 4f). All rats exposed to PHMG-phosphate aerosol particles showed slight inflammatory and fibrotic responses (score 2) in their lung tissues (Table 4).

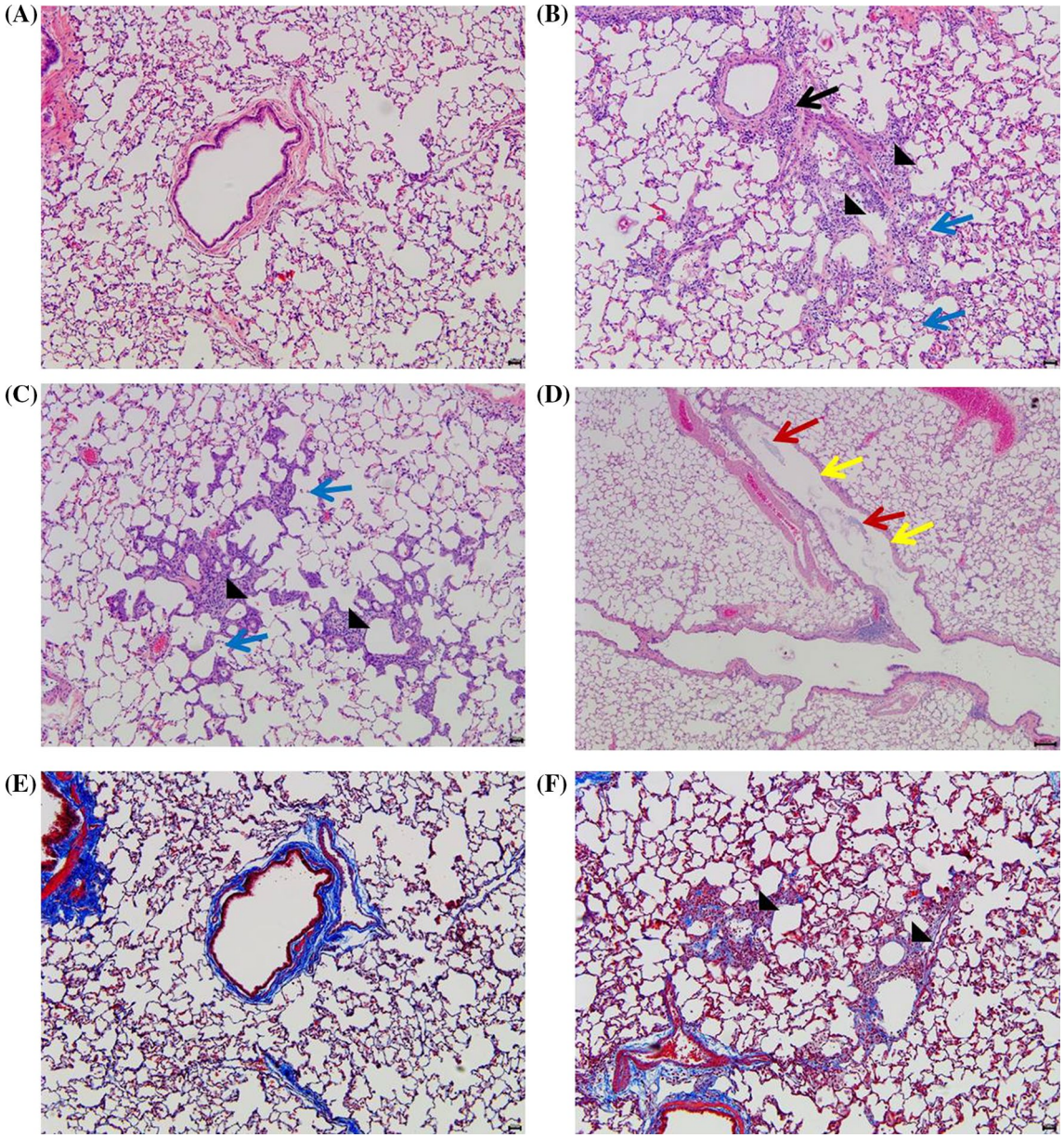


**Fig. 4** Effect of PHMG-phosphate aerosol particles on lung histology in rats. Representative photomicrographs of lung sections stained with H&E (**a**–**d**) and Masson's trichrome (**e**, **f**). Lung sections of rats exposed to clean air (**a**, **e**) and PHMG-phosphate aerosol particles (**b**–**d**, **f**). *Black arrow* inflammatory cell infiltration, *triangle* fibrosis, *blue arrow* foamy histiocytes, *red arrow* mucus plug, *yellow arrow* atrophy/necrosis of bronchiolar epithelium. Magnification: ×100, bar: 50 μm (color figure online)

## Effect of PHMG-phosphate on ROS generation in a bronchial ALI co-culture model

The determination of intracellular ROS generation in a bronchial ALI co-culture model by DCFH-DA method showed that PHMG-phosphate increased the DCF fluorescence intensity in a dose-dependent manner after 3-h exposure (Fig. 5). The ROS generation in the cells treated with 35.1 mg/ml PHMG-phosphate was 143 % in comparison with the vehicle control.

## Effect of PHMG-phosphate on an airway barrier injury in a bronchial ALI co-culture model

PHMG-phosphate significantly decreased the cell viability in the bronchial ALI co-culture model (Fig. 6). $LC_{50}$ values at 1-, 6- and 24-h exposure were 8.8, 8.8 and 4.4 mg/ml, respectively. Barrier integrity and function collapsed dose-dependently by 24-h exposure of PHMG-phosphate. The permeability of the airway barrier in a bronchial ALI co-culture model was assessed by measuring the FITC-dextran

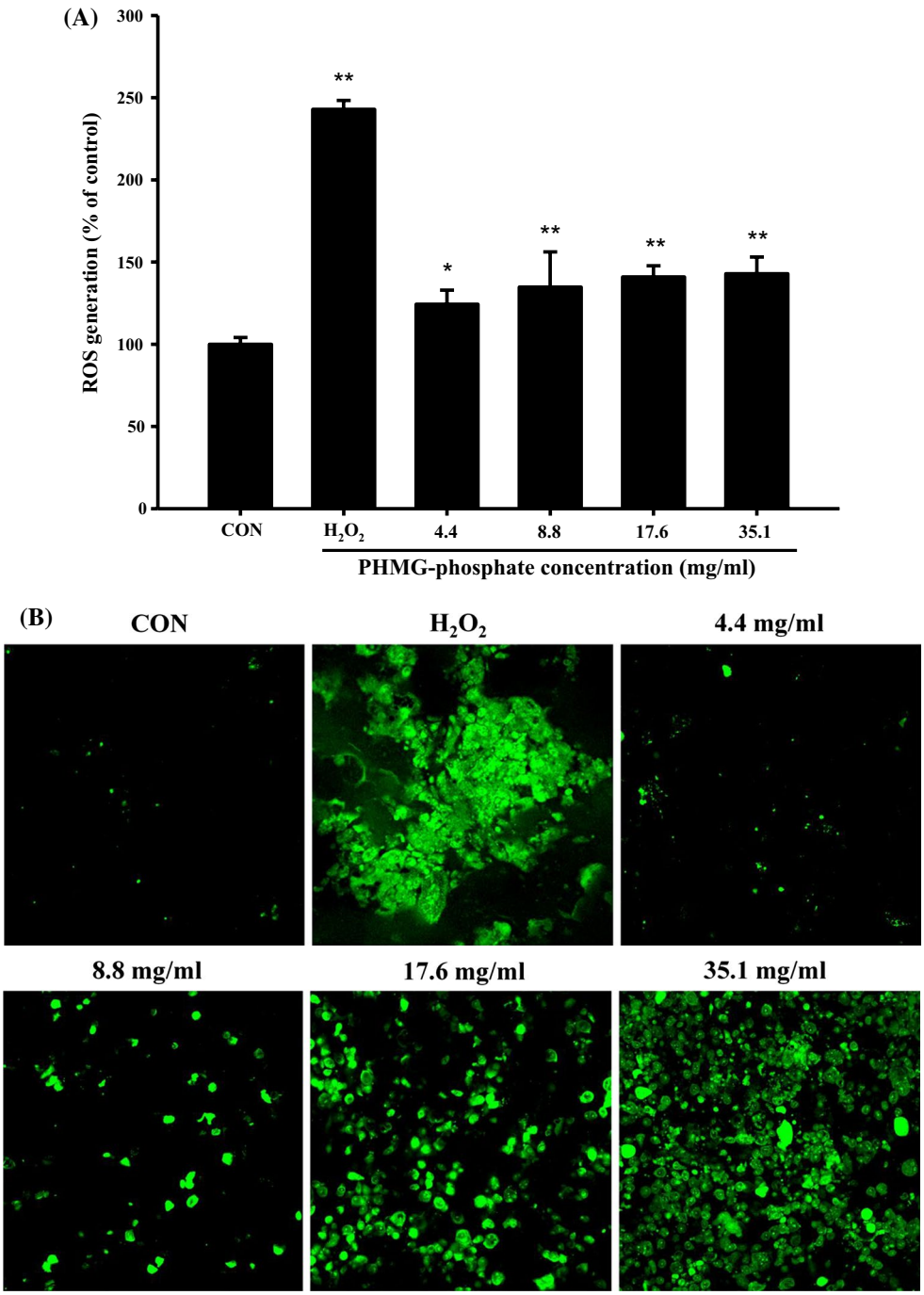


**Fig. 5** Effect of PHMG-phosphate on reactive oxygen species (ROS) generation in a bronchial ALI co-culture model. The cells were incubated with PHMG-phosphate for 3 h. **a** ROS was detected by fluorescence measurement of the reported DCF, and the result is given as percent to the vehicle control (CON). The results are expressed as mean ± SD of three separate experiments for each data point. Values are significantly different from CON: $*p < 0.05$; $**p < 0.01$. **b** ROS generation was visualized by fluorescence observation (×200, *light green*) (color figure online)

paracellular flux (Fig. 7a). The permeability of 40 kDa FITC-dextran was dose-dependently increased by PHMG-phosphate. The permeability dramatically increased up to 596.11 ± 149.57 % at the highest concentration compared with the control. TEER decreased dose-dependently (Fig. 7b). TEER was 13.73 ± 4.14 Ohm × $cm^2$ in co-culture cells exposed to 17.6 mg/ml of PHMG-phosphate, showing 3.87 ± 1.17 % of control. A dose-dependent disruption of E-cadherin (light green) was observed by the immunofluorescence method (Fig. 7c). E-cadherin seemed to show no significant difference with control until the exposure of PHMG-phosphate 2.2 mg/ml. However, E-cadherin showed faded green and dark space becoming larger at a higher concentration than 2.2 mg/ml.

The mRNA levels of MMP-2, MMP-9, TIMP-1 and TIMP-2 were assessed in co-culture cells exposed to PHMG-phosphate 4.4 mg/ml for 1, 6 and 24 h. The mRNA of MMP-2 was significantly enhanced to 4.76-, 4.06- and 5.33-fold induction in all indicated time periods, respectively (Fig. 8a). The MMP-9 mRNA expression

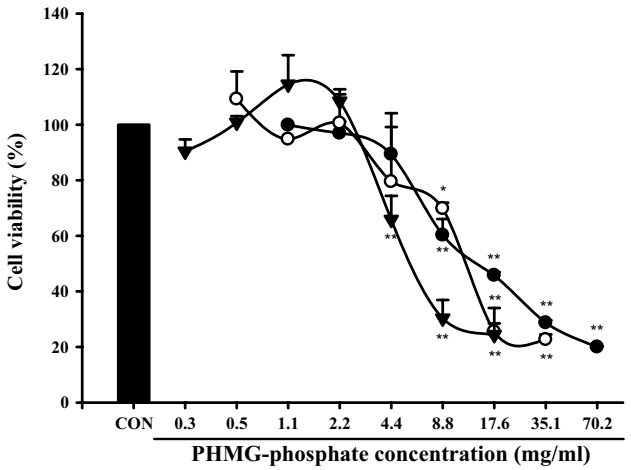


**Fig. 6** Cell viability in a bronchial ALI co-culture model. The cells were incubated with PHMG-phosphate for 1 h (*black circles*), 6 h (*white circles*) or 24 h (*triangle*). WST-1 assays were carried out. The results are expressed as mean ± SD of three separate experiments for each data point. Values are significantly different from the vehicle control (CON): $*p < 0.05$; $**p < 0.01$

was significantly up-regulated by 7.26-fold induction on 24-h exposure, while other time periods showed a low-fold change (Fig. 8b). The mRNA expression of following inhibitors of MMPs was also increased. The TIMP-1 and TIMP-2 mRNA expressions were time dependently increased and were significantly up-regulated by 4.00- and 11.76-fold on 24-h exposure, respectively (Fig. 8c, d).

### Effect of PHMG-phosphate on profibrotic inflammatory responses in a bronchial ALI co-culture model

The regulation of cytokines was assessed by ELISA assay to find out the profibrotic inflammatory responses of PHMG-phosphate. Co-culture cells exposed to PHMG-phosphate for 1, 6 and 24 h significantly up-regulated the levels of TNF-α, IL-6, IL-8 and TGF-β. The level of TNF-α, which was the smallest among the cytokines, showed little difference between the concentrations and the amount of TNF-α (Fig. 9a). The levels of IL-6 and IL-8 significantly showed a dose-dependent increase by PHMG-phosphate (Fig. 9b, c). PHMG-phosphate secreted TGF-β significantly at relatively lower concentrations compared with other cytokine secretions (Fig. 9d). As longer the exposure time of PHMG-phosphate, as higher the levels of TNF-α, IL-6, IL-8 and TGF-β.

## Discussion

With an increasing use of humidifier to prevent excessive drying and to maintain comfortable room humidity, human health effects of aerosol particles released from humidifier become important. Previous studies showed that ultrasonic humidifier may release dissolved particles with nanometers in size (Rodes et al. 1990). Particles with approximately 20–60 nm diameters were found in lung macrophages if they were exposed to aerosol that was released from humidifier. Those aerosol particles consist of minerals and initiate dysregulation of genes related to mitosis, cell adhesion molecules, major histocompatibility complex molecules and endocytosis. However, aerosol particles released from humidifier did not induce any signs of inflammation or tissue injury in mice lungs (Umezawa et al. 2013). In Korea, manufacturers innovatively extended the usage of PHMG-phosphate, which has been registered as a medical device disinfectant by the United States Food and Drug Administration. PHMG-phosphate was added to humidifier water in order to prevent the growth of harmful bacteria, mold and algae and was called as "humidifier disinfectant" product. Epidemiological studies reported that prolonged inhalation of aerosol released from humidifier to put a commercial disinfectant can provoke pulmonary fibrosis. It was supposed that PHMG-phosphate might be reconstituted as a solid particle form adsorbed on dissolved minerals with nanometers in size, facilitating infiltrates into deep pulmonary bronchiole where their toxic effects manifest.

First, we conducted an in vivo study to identify whether PHMG-phosphate aerosol particles with an atmospheric concentration considering the patient exposure profile induce inflammatory and fibrotic responses in lungs. According to the epidemiological survey (Kim et al. 2014a, b; Hong et al. 2014), the patients used a humidifier for over 8 h a day during 4 months and showed the incidence of pulmonary disease in March almost at the end of winter. The maximum incidence rate was shown at the end of April. Patients in intensive care ($n = 10$) died ($n = 5$) or got a lung transplantation ($n = 5$). The atmosphere concentration of PHMG-phosphate aerosol particles was about 0.1 mg/m$^3$ according to our preliminary study with the recommended usage of product (KCDC 2011). Therefore, the exposure conditions for PHMG-phosphate aerosol particles in this study were decided by us to 1.5 mg/m$^3$, 4 h/day and 5 days/week during 3 weeks based on those scenarios of hospitalized patients. In addition, we added a recover period of 3 weeks, considering patient's circumstances and observed clinical signs, body weight and respiration rate. After all, rats were exposed to 1.51 mg/m$^3$ PHMG-phosphate aerosol particles with 93.35 nm in size for 3 weeks and recovered for 3 weeks in a nose-only exposure chamber (Fig. 1; Table 2). All animals showed an irregular respiration and a decrease in its mobility at the end of 3-week exposure. Also, the body weight was decreased at the end of the exposure and reached almost 75 % of control animals similar to moribund right before

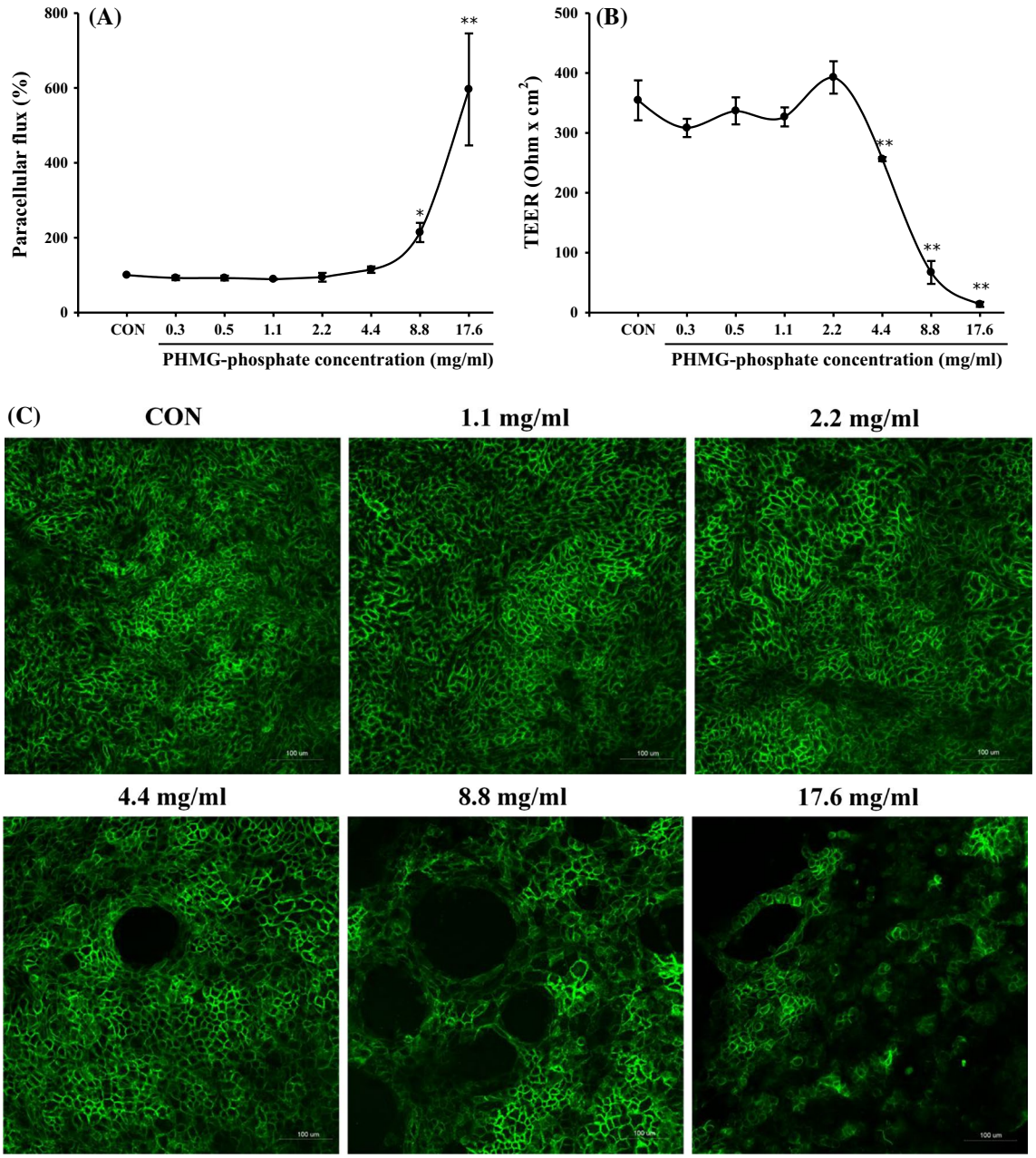


**Fig. 7** Disruption of the epithelial airway barrier by PHMG-phosphate in a bronchial ALI co-culture model. The co-culture cells seeded into transwell inserts were incubated with 1.1–17.6 mg/ml of PHMG-phosphate for 24 h. **a** The permeability of the airway barrier was evaluated by measuring the FITC-dextran paracellular flux. The result is given as percent to the vehicle control (CON). **b** Effect of PHMG-phosphate on transepithelial electrical resistance (TEER). The results are expressed as mean ± SD of three separate experiments for each data point. Values are significantly different from control: $*p < 0.05$; $**p < 0.01$. **c** Immunoblotting of E-cadherin (×200; *light green*) (color figure online)

necropsy (Fig. 2). The rats exposed to PHMG-phosphate aerosol particles showed a 2.6 times higher respiration rate than the control animals with a sustained respiration function decrease without an additional exposure to PHMG-phosphate aerosol particles (Table 3). Patients had been continuously aggravated under intensive care in the hospital after quitting humidifier. Our in vivo data are consistent with clinical signs in hospitalized patients, which may be injured by a humidifier disinfectant.

The IL-1β and IL-6 significantly increased (Fig. 3a), and the quantitative evaluation on inflammation showed a score of 2 in the exposure group (Table 4). In particular, the fibronectin mRNA was up-regulated (Fig. 3b), and histologic observations were detected related to lung fibrosis

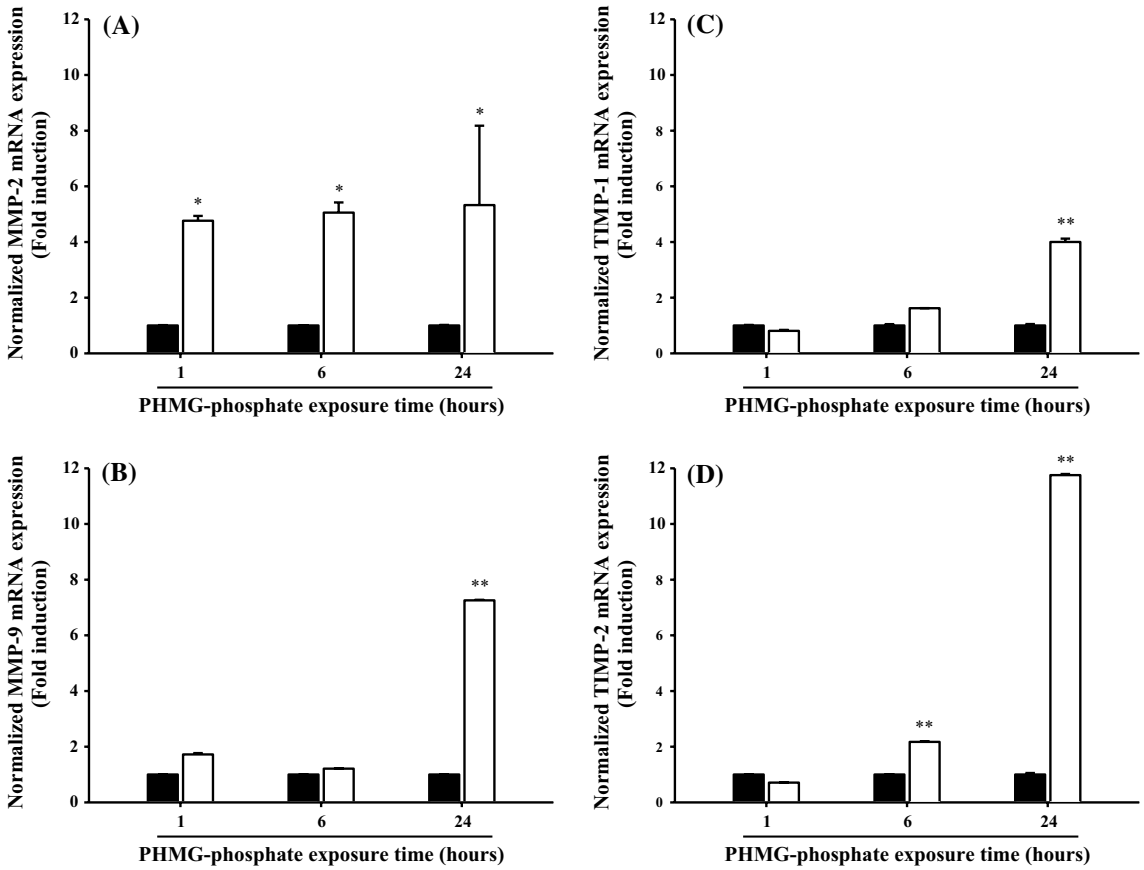


**Fig. 8** Regulation of MMP-2, MMP-9, TIMP-1 and TIMP-2 mRNA levels by PHMG-phosphate in a bronchial ALI co-culture model. PHMG-phosphate induced mRNA levels of MMP-2 (**a**), MMP-9 (**b**), TIMP-1 (**c**) and TIMP-2 (**d**). Real-time PCR was performed after 1-, 6- and 24-h incubation with PHMG-phosphate 4.4 mg/ml in co-culture cells. The results are normalized to 18 s RNA and are given as fold induction to control. The control or exposure groups represent a *black* or *white bar*, respectively. The results are expressed as mean ± SD of three separate experiments for each data point. Values are significantly different from control: $*p < 0.05$; $**p < 0.01$

such as mucus plug and collagen accumulation (Fig. 4d, f). Those results demonstrate that lung damage was not recovered by nose-only exposure of PHMG-phosphate aerosol particles for 3 weeks and led to a progress of inflammation and fibrosis in lungs. According to the epidemiological study of Kim et al. (2014b), common pathologic features shown in hospitalized patients were variable degrees of a bronchiolar injury. In most of the cases, the fibrotic inflammatory process was temporally homogeneous. In early lesions, the bronchiolar epithelium was denuded or replaced by flattened epithelium. The late phase was characterized by the centrilobular distribution of a parenchymal remodeling caused by septal inflammation, fibroblastic proliferation, collagen deposition and intra-alveolar fibroblastic plugs with mural incorporation. Histopathological findings from hospitalized patients were reproduced in our in vivo animal experiment with strong evidences related to inflammation and fibrosis on the molecular level.

We elucidated the fibrogenesis mechanism of PHMG-phosphate in a bronchial ALI co-culture model. The ALI co-culture model of the human epithelial airway barrier is composed of epithelial cells and the two most important immune cells and represents the conditions that would be expected in the human lung. Epithelial cells are important to maintain the lung functionality such as forming a barrier against pathogens and other harmful compounds, promoting mucociliary clearance and secreting protective substances (Proud 2008). Macrophages are specialized defense cells and ingest foreign particles by phagocytosis. Moreover, mast cells are an important element of the lung airway structure, which mainly secret histamine and play a role in the innate immune system (Klein et al. 2013). An interaction between bronchial epithelial cells, macrophages and mast cells increases the toxic responses to particulate the matter (Ishii et al. 2005; Alfaro-Moreno et al. 2008; Val et al. 2012). Recently, a co-culture model at ALI cultivation was applied for the evaluation of toxic effects of inhalable particles (Diabaté et al. 2008; Brandenberger et al. 2010). After all, the ALI co-culture model could provide a better understanding for toxic mechanisms of foreign compounds

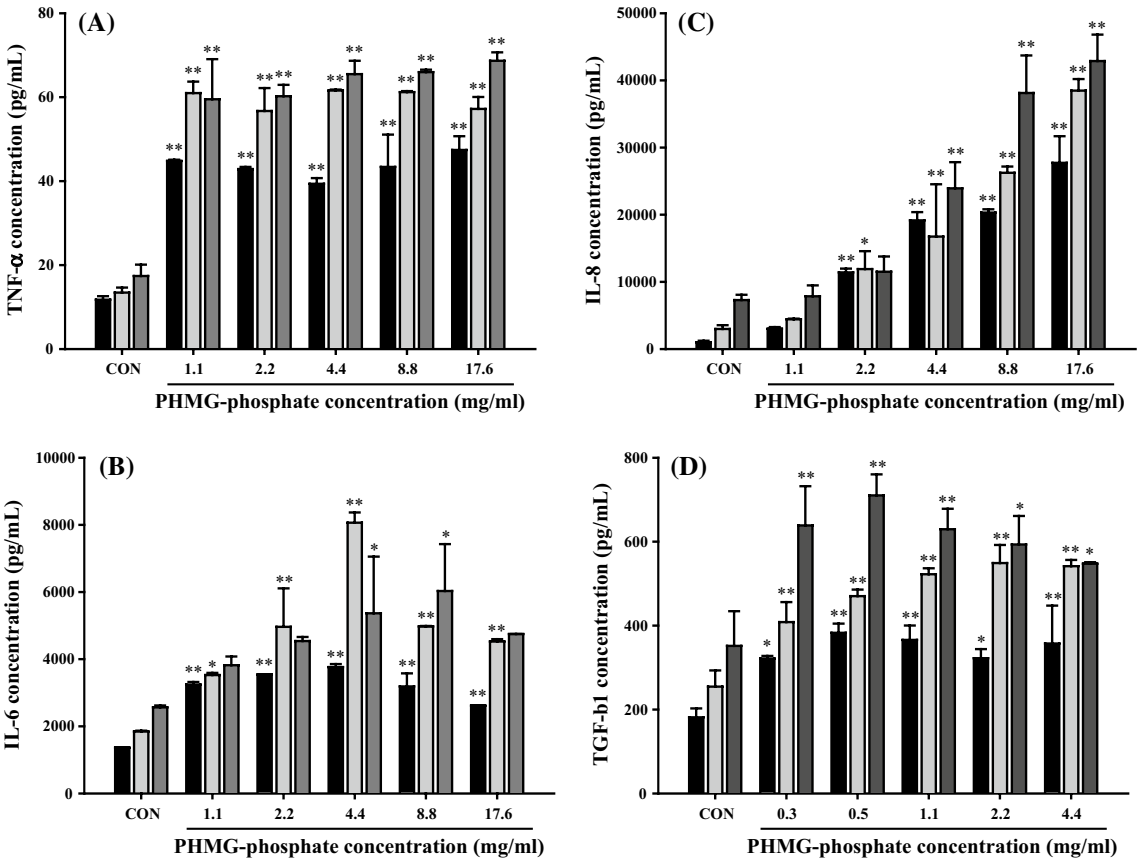


**Fig. 9** TNF-α, IL-6, IL-8 and TGF-β secretions by PHMG-phosphate in a bronchial ALI co-culture model. PHMG-phosphate significantly enhanced TNF-α (**a**), IL-6 (**b**), IL-8 (**c**) and TGF-β (**d**), which are profibrotic inflammatory cytokines. Supernatants were collected after 1-(*black bar*), 6-(*gray bar*) and 24-h (*dark gray bar*) treatment of PHMG-phosphate in co-culture cells. Then, an ELISA assay was performed to capture the release of cytokines. The results are expressed as mean ± SD of three separate experiments for each data point. Values are significantly different from CON: $*p < 0.05$; $**p < 0.01$

due to more realistic in vitro circumstances regarding to the respiratory tract. However, there are few reports using the ALI co-culture model yet. In the present study, we used three cell types: Calu-3, a bronchial epithelial cell; THP-1, a monocyte cell; and HMC-1, a mast cell. The Calu-3 cells cultured at ALI produce a cell layer with greater similarity to the in vivo airway epithelial morphology such as ciliogenesis, mucus secretion and tight junction formation (Grainger et al. 2006). For that reason, Calu-3 cell line has become a popular model for studying the toxicology in airway (Shan et al. 2011).

A fibrosis mechanism is described as wound-healing response, which is composed of three distinct phases (i.e., injury, inflammation and repair), and it has been a useful model to elucidate the common and divergent mechanisms of pulmonary fibrosis (Wilson and Wynn 2009). An injury of epithelial cells often results in the disruption of normal tissue architecture, which initiates a wound-healing response. First of all, PHMG-phosphate significantly produced ROS in the bronchial ALI co-culture model (Fig. 5). Oxidant–antioxidant imbalances in the lower respiratory tract play a critical role in fibrogenesis (Kinnula et al. 2005). Bleomycin has been known for causing lung injury via ROS generation. It forms a DNA/$Fe^{2+}$/bleomycin complex, which undergoes redox cycling and generates ROS including superoxide and hydroxyl radicals (Hay et al. 1991; Giri 2003). Asbestos also increased ROS directly via transition metal reactions and indirectly via oxidative burst from recruited macrophages (Hansen and Mossman 1987). PHMG-phosphate dose-dependently decreased the cell viability in a bronchial ALI co-culture model (Fig. 6). The amount of FITC-dextran was dose-dependently increased by PHMG-phosphate. This is indicated as disruption of the cell–cell junction to maintain the function of paracellular permeability in the airway (Fig. 7a). The barrier integrity evaluated by TEER showed a dose-dependent decrease (Fig. 7b). In addition, PHMG-phosphate induced a breakage of E-cadherin, which plays an important role in the development and maintenance of junctional complexes (Fig. 7c). These results indicate that PHMG-phosphate

destroys the barrier integrity and cell–cell junction. The balance between MMPs and TIMPs in lung is a responsible factor in the inflammation and for the amount of net collagen deposition during the wound-healing response (Pardo and Selman 2006). The abnormal collagenolysis by MMPs was suspected to be an excess accumulation of ECM in the pulmonary fibrosis. Expression of MMP-9 tends to occur in the early stage of pulmonary fibrosis because it is mainly derived from macrophages (Lemjabbar et al. 1999), while MMP-2 seems to increase in the late stage of the disease (Fukuda et al. 1998). MMP-2 and MMP-9 are inhibited by TIMP-2 and TIMP-1, respectively. TIMP-1 is also produced with the stages of fibrosis progression and may prevent a MMP-induced ECM degradation and consequently could take part in the accumulation of ECM (Lemjabbar et al. 1999). TIMP-2 not only inhibits MMP-2, but also, paradoxically, influences the MMP-2 elevation by binding to pro-MMP-2 (Selman et al. 2000). Hayashi et al. (1996) reported that MMP-2, MMP-9, TIMP-1 and TIMP-2 are enhanced at the damage site of alveolar and at disrupted membranes in patients with idiopathic pulmonary fibrosis. Moreover, in rats exposed to paraquat or bleomycin, the increase of MMP-2 and MMP-9 mRNA expression reached its peak at day 7, while TIMP-1 and TIMP-2 mRNA levels reached the peak on 14–21 days after exposure (Oggionni et al. 2009; Wang et al. 2011). The regulation of MMP-2, MMP-9, TIMP-1 and TIMP-2 mRNA by PHMG-phosphate is consistent with the results of paraquat and bleomycin studies. The mRNA levels of MMP-2, MMP-9, TIMP-1 and TIMP-2 were significantly elevated in co-culture cells exposed to 4.4 mg/ml PHMG-phosphate for 24 h (Fig. 8). Those results indicate that PHMG-phosphate may destruct the basement membrane, which could lead to severe damage of the lung architecture and aberrant ECM deposition. The imbalance of MMPs and TIMPs caused by PHMG-phosphate could lead to a failure of re-epithelialization and promote the migration of fibroblasts/myofibroblasts into the lung. Taken together, PHMG-phosphate induced an airway barrier injury as initiation of a wound-healing response.

Numerous inflammatory cytokines are released after epithelium injury, and some of them are related to the fibrogenesis. The ROS can activate redox-sensitive transcription factors including nuclear factor kappa B and produce inflammatory cytokines. TNF-α is directly or indirectly associated with wound-healing and tissue-remodeling as it induces IL-6, IL-8 and TGF-β (Schröder et al. 1990; Warshamana et al. 2001). TNF-α can be a relevant inflammatory marker and also can stimulate fibroblast activation and collagen synthesis in vitro (Piguet et al. 1989). Both IL-6 and IL-8 can stimulate fibrogenesis due to collagen production and angiogenic activity (Duncan and Berman 1991; Keane et al. 1997). TGF-β has been found most effectively to accelerate fibrosis in the lung through mediating epithelial–mesenchymal transition, which means that epithelial differentiates to myofibroblast, is chemoattracting for fibroblasts, promotes the fibroblast pro-collagen gene expression, inhibits the collagen degradation, and partially affects the elevation of TIMP-1 (Kolb et al. 2001; Bonner 2010; Chapman 2011). We measured the amount of inflammatory cytokines in the bronchial ALI co-culture model. PHMG-phosphate significantly induced TNF-α, IL-6, IL-8 and TGF-β (Fig. 9), and those in vitro data indicate that PHMG-phosphate induced fibrotic inflammatory responses in bronchial ALI co-culture model.

In conclusion, PHMG-phosphate aerosol particles induced a pulmonary inflammation and fibrosis including an increase in inflammatory cytokines and fibronectin mRNA, as well as histopathological changes in rats. All features of fibrogenesis by PHMG-phosphate aerosol particles closely resembled the pathology of fibrosis reported in epidemiological studies on the use of humidifier containing disinfectants. Moreover, PHMG-phosphate triggered the ROS generation, airway barrier injury and inflammatory responses in the bronchial ALI co-culture model. Finally, we expected that PHMG-phosphate infiltrated into the lungs in form of aerosol particles would induce an airway barrier injury via ROS, release fibrotic inflammatory cytokines, and trigger a wound-healing response, leading to pulmonary fibrosis. A simultaneous state of tissue destruction and inflammation caused by PHMG-phosphate has whipped up a "perfect storm" in the respiratory tract of humans, directing damage to consumers, their children and their family.

**Acknowledgments** This work was partly supported by the Korea Environmental Industry and Technology Institute (Grant Number: 2012001370006).

## References

Aleshina EY, Yudanova TN, Skokova IF (2001) Production and properties of polyvinyl alcohol spinning solutions containing protease C and polyhexamethylene guanidine. Fibre Chem 33:421–423

Alexander DJ, Collins CJ, Coombs DW, Gilkison IS, Hardy CJ, Healey G, Karantabias G, Johnson N, Karlsson A, Kilgour JD, McDonald P (2008) Association of Inhalation Toxicologists (AIT) working party recommendation for standard delivered dose calculation and expression in non-clinical aerosol inhalation toxicology studies with pharmaceuticals. Inhal Toxicol 20:1179–1189

Alfaro-Moreno E, Nawrot TS, Vanaudenaerde BM, Hoylaerts MF, Vanoirbeek JA, Nemery B, Hoet PH (2008) Co-cultures of multiple cell types mimic pulmonary cell communication in response to urban PM10. Eur Respir J 32:1184–1194

Bonner JC (2008) Respiratory toxicity. In: Smart RC, Hodgson E (eds) Molecular and biochemical toxicology, 4th edn. Wiley, New York, pp 639–670

Bonner JC (2010) Mesenchymal cell survival in airway and interstitial pulmonary fibrosis. Fibrogenesis Tissue Repair 3:15

Brandenberger C, Rothen-Rutishauser B, Mühlfeld C, Schmid O, Ferron GA, Maier KL, Gehr P, Lenz AG (2010) Effects and uptake of gold nanoparticles deposited at the air-liquid interface of a human epithelial airway model. Toxicol Appl Pharmacol 242:56–65

Chapman HA (2011) Epithelial-mesenchymal interactions in pulmonary fibrosis. Annu Rev Physiol 73:413–435

Diabaté S, Mülhopt S, Paur HR, Krug HF (2008) The response of a co-culture lung model to fine and ultrafine particles of incinerator fly ash at the air-liquid interface. Altern Lab Anim 36:285–298

Duncan MR, Berman B (1991) Stimulation of collagen and glycosaminoglycan production in cultured human adult dermal fibroblasts by recombinant human interleukin 6. J Invest Dermatol 97:686–692

Fukuda Y, Ishizaki M, Kudoh S, Kitaichi M, Yamanaka N (1998) Localization of matrix metalloproteinases-1,-2, and-9 and tissue inhibitor of metalloproteinase-2 in interstitial lung diseases. Lab Invest 78:687–698

Gilbert P, Moore LE (2005) Cationic antiseptics: diversity of action under a common epithet. J Appl Microbiol 99:703–715

Giri SN (2003) The combined treatment with taurine and niacin blocks the bleomycin-induced activation of nuclear factor-kappaB and lung fibrosis. Adv Exp Med Biol 526:381–394

Gorguner M, Aslan S, Inandi T, Cakir Z (2004) Reactive airways dysfunction syndrome in housewives due to a bleach-hydrochloric acid mixture. Inhal Toxicol 16:87–91

Grainger CI, Greenwell LL, Lockley DJ, Martin GP, Forbes B (2006) Culture of Calu-3 cells at the air interface provides a representative model of the airway epithelial barrier. Pharm Res 23:1482–1490

Hansen K, Mossman BT (1987) Generation of superoxide (O2-.) from alveolar macrophages exposed to asbestiform and nonfibrous particles. Cancer Res 47:1681–1686

Hay J, Shahzeidi S, Laurent G (1991) Mechanisms of bleomycin-induced lung damage. Arch Toxicol 65:81–94

Hayashi T, Stetler-Stevenson WG, Fleming MV, Fishback N, Koss MN, Liotta LA, Ferrans VJ, Travis WD (1996) Immunohistochemical study of metalloproteinases and their tissue inhibitors in the lungs of patients with diffuse alveolar damage and idiopathic pulmonary fibrosis. Am J Pathol 149:1241–1256

Heinzer R, Ribordy V, Kuzoe B, Lazor R, Fitting JW (2004) Recurrence of acute respiratory failure following use of waterproofing sprays. Thorax 59:541–542

Herzog F, Clift MJ, Piccapietra F, Behra R, Schmid O, Petri-Fink A, Rothen-Rutishauser B (2013) Exposure of silver-nanoparticles and silver-ions to lung cells in vitro at the air-liquid interface. Part Fibre Toxicol 10:11. doi:10.1186/1743-8977-10-11

Hong SB, Kim HJ, Huh JW, Do KH, Jang SJ, Song JS, Choi SJ, Heo Y, Kim YB, Lim CM, Chae EJ, Lee H, Jung M, Lee K, Lee MS, Koh Y (2014) A cluster of lung injury associated with home humidifier use: clinical, radiological and pathological description of a new syndrome. Thorax. doi:10.1136/thoraxjnl-2013-204135

Ishii H, Hayashi S, Hogg JC, Fujii T, Goto Y, Sakamoto N, Mukae H, Vincent R, van Eeden SF (2005) Alveolar macrophage-epithelial cell interaction following exposure to atmospheric particles induces the release of mediators involved in monocyte mobilization and recruitment. Resp Res 6:87

Kacmarek RM, Stoller JK, Heuer AH (2013) Egan's fundamentals of respiratory care, 10th edn. Mosby, St. Louis

Keane MP, Arenberg DA, Lynch JP 3rd, Whyte RI, Iannettoni MD, Burdick MD, Wilke CA, Morris SB, Glass MC, DiGiovine B, Kunkel SL, Strieter RM (1997) The CXC chemokines, IL-8 and IP-10, regulate angiogenic activity in idiopathic pulmonary fibrosis. J Immunol 159:1437–1443

Kim JY, Kim HH, Cho KH (2013) Acute cardiovascular toxicity of sterilizers, PHMG, and PGH: severe inflammation in human cells and heart failure in zebrafish. Cardiovasc Toxicol 13:148–160

Kim HJ, Lee MS, Hong SB, Huh JW, Do KH, Jang SJ, Lim CM, Chae EJ, Lee H, Jung M, Park YJ, Park JH, Kwon GY, Gwack J, Youn SK, Kwon JW, Yang BG, Jun BY, Kim Y, Cheong HK, Chun BC, Kim H, Lee K, Koh Y (2014a) A cluster of lung injury cases associated with home humidifier use: an epidemiological investigation. Thorax. doi: 10.1136/thoraxjnl-2013-204132

Kim KW, Ahn K, Yang HJ, Lee S, Park JD, Kim WK, Kim JT, Kim HH, Rha YH, Park YM, Sohn MH, Oh JW, Lee HR, Lim DH, Choung JT, Han MY, Lee E, Kim HY, Seo JH, Kim BJ, Cho YA, Do KH, Kim SA, Jang SJ, Lee MS, Kim HJ, Kwon GY, Park JH, Gwack J, Youn SK, Kwon JW, Jun BY, Pyun BY, Hong SJ (2014b) Humidifier disinfectant-associated children's interstitial lung disease. Am J Respir Crit Care Med 189:48–56

Kinnula VL, Fattman CL, Tan RJ, Oury TD (2005) Oxidative stress in pulmonary fibrosis: a possible role for redox modulatory therapy. Am J Respir Crit Care Med 172:417–422

Klein SG, Serchi T, Hoffmann L, Blömeke B, Gutleb AC (2013) An improved 3D tetraculture system mimicking the cellular organisation at the alveolar barrier to study the potential toxic effects of particles on the lung. Part Fibre Toxicol 10:31. doi:10.1186/1743-8977-10-31

Kolb M, Margetts PJ, Anthony DC, Pitossi F, Gauldie J (2001) Transient expression of IL-1beta induces acute lung injury and chronic repair leading to pulmonary fibrosis. J Clin Invest 107:1529–1536

Korea Centers for Disease Control and Prevention (2011) Interim report of epidemiological investigation on lung injury with unknown cause in Korea. Public Health Weekly Report KCDC 4:817–832 (In Korean). Accessed 26 July 2012

Lemjabbar H, Gosset P, Lechapt-Zalcman E, Franco-Montoya ML, Wallaert B, Harf A, Lafuma C (1999) Overexpression of alveolar macrophage gelatinase B (MMP-9) in patients with idiopathic pulmonary fibrosis: effects of steroid and immunosuppressive treatment. Am J Respir Cell Mol Biol 20:903–913

Limper AH, Broekelmann TJ, Colby TV, Malizia G, McDonald JA (1991) Analysis of local mRNA expression for extracellular matrix proteins and growth factors using in situ hybridization in fibroproliferative lung disorders. Chest 99(Suppl 3):55S–56S

Matsui H, Verghese MW, Kesimer M, Schwab UE, Randell SH, Sheehan JK, Grubb BR, Boucher RC (2005) Reduced three-dimensional motility in dehydrated airway mucus prevents neutrophil capture and killing bacteria on airway epithelial surfaces. J Immunol 175:1090–1099

Oggionni T, Morbini P, Inghilleri S, Palladini G, Tozzi R, Vitulo P, Fenoglio C (2009) Time course of matrix metalloproteases and tissue inhibitors in bleomycin-induced pulmonary fibrosis. Eur J Histochem 50:317–326

Oulé MK, Quinn K, Dickman M, Bernier AM, Rondeau S, De Moissac D, Boisvert A, Diop L (2012) Akwaton, polyhexamethyleneguanidine hydrochloride-based sporicidal disinfectant: a novel tool to fight bacterial spores and nosocomial infections. J Med Microbiol 61:1421–1427

Pardo A, Selman M (2006) Matrix metalloproteases in aberrant fibrotic tissue remodeling. Proc Am Thorac Soc 3:383–388

Piguet PF, Collart MA, Grau GE, Kapanci Y, Vassalli P (1989) Tumor necrosis factor/cachectin plays a key role in bleomycin-induced pneumopathy and fibrosis. J Exp Med 170:655–663

Proud D (2008) The pulmonary epithelium in health and disease. Wiley, New York

Reagan-Shaw S, Nihal M, Ahmad N (2008) Dose translation from animal to human studies revisited. FASEB J 22:659–661

Rodes C, Smith T, Crouse R, Ramachandran G (1990) Measurements of the size distribution of aerosols produced by ultrasonic humidification. Aerosol Sci Tech 13:220–229

Schröder JM, Sticherling M, Henneicke HH, Preissner WC, Christophers E (1990) IL-1 alpha or tumor necrosis factor-alpha

stimulate release of three NAP-1/IL-8-related neutrophil chemotactic proteins in human dermal fibroblasts. J Immunol 144:2223–2232

Selman M, Ruiz V, Cabrera S, Segura L, Ramírez R, Barrios R, Pardo A (2000) TIMP-1,-2,-3, and-4 in idiopathic pulmonary fibrosis. A prevailing nondegradative lung microenvironment? Am J Physiol Lung Cell Mol Physiol 279:L562–L574

Shan J, Huang J, Liao J, Robert R, Hanrahan JW (2011) Anion secretion by a model epithelium: more lessons from Calu-3. Acta Physiol (Oxf) 202:523–531

Song JA, Park HJ, Yang MJ, Jung KJ, Yang HS, Song CW, Lee K (2014) Polyhexamethyleneguanidine phosphate induces severe lung inflammation, fibrosis, and thymic atrophy. Food Chem Toxicol 69:267–275

Umezawa M, Sekita K, Suzuki K, Kubo-Irie M, Niki R, Ihara T, Sugamata M, Takeda K (2013) Effect of aerosol particles generated by ultrasonic humidifiers on the lung in mouse. Part Fibre Toxicol 10:64. doi:10.1186/1743-8977-10-64

Val S, Belade E, George I, Boczkowski J, Baeza-Squiban A (2012) Fine PM induce airway MUC5AC expression through the autocrine effect of amphiregulin. Arch Toxicol 86:1851–1859

Wang BL, Tu YY, Fu JF, Zhong YX, Fu GQ, Tian XX, Wang LH, Gong L, Ren QY (2011) Unbalanced MMP/TIMP-1 expression during the development of experimental pulmonary fibrosis with acute paraquat poisoning. Mol Med Rep 4:243–248

Warshamana GS, Corti M, Brody AR (2001) TNF-alpha, PDGF, and TGF-beta(1) expression by primary mouse bronchiolar-alveolar epithelial and mesenchymal cells: tnf-alpha induces TGF-beta(1). Exp Mol Pathol 71:13–33

Wilson MS, Wynn TA (2009) Pulmonary fibrosis: pathogenesis, etiology and regulation. Mucosal Immunol 2:103–121

Wynn TA (2011) Integrating mechanisms of pulmonary fibrosis. J Exp Med 208:1339–1350

Zock JP, Plana E, Jarvis D, Antó JM, Kromhout H, Kennedy SM, Künzli N, Villani S, Olivieri M, Torén K, Radon K, Sunyer J, Dahlman-Hoglund A, Norbäck D, Kogevinas M (2007) The use of household cleaning sprays and adult asthma: an international longitudinal study. Am J Respir Crit Care Med 176:735–741